HHS Public Access

Author manuscript

J Immunol. Author manuscript; available in PMC 2023 February 01.

Published in final edited form as:

J Immunol. 2022 August 01; 209(3): 621–628. doi:10.4049/jimmunol.2200041.

PPP2R2D suppresses effector T cell exhaustion and Treg expansion and inhibits tumor growth in melanoma

Wenliang Pan[*], **Marc Scherlinger**[*], **Nobuya Yoshida**[*], **Maria G. Tsokos**[*], **George C. Tsokos**[*,†]

[*]Department of Medicine, Beth Israel Deaconess Medical Center, Harvard Medical School, Boston, Massachusetts, USA.

Abstract

We had shown previously that the PP2A regulatory subunit PPP2R2D suppresses IL-2 production and PPP2R2D deficiency in T cells potentiates the suppressive function of regulatory T (Treg) cells and alleviates imiquimod-induced lupus-like pathology. Here in a melanoma xenograft model we noted that the tumor grew in larger sizes in mice lacking PPP2R2D in T cells ($Lck^{Cre}R2D^{fl/fl}$) compared to wild type ($R2D^{fl/fl}$) mice. The numbers of intratumoral T cells in $Lck^{Cre}R2D^{fl/fl}$ mice were reduced compared to $R2D^{fl/fl}$ mice and they expressed a $PD\text{-}1^{+}CD3^{+}CD44^{+}$ exhaustion phenotype. *In vitro* experiments confirmed that the chromatin of exhaustion markers PD-1, LAG3, TIM3 and CTLA4 remained open in $Lck^{Cre}R2D^{fl/fl}$ CD4 T conventional (Tconv) compared to $R2D^{fl/fl}$ Tconv cells. Moreover, the percentage of Treg cells ($CD3^{+}CD4^{+}FoxP3^{+}CD25^{hi}$) was significantly increased in the xenografted tumor of $Lck^{Cre}R2D^{fl/fl}$ mice compared to $R2D^{fl/fl}$ mice probably because of the increase in the percentage of IL-2-producing $Lck^{Cre}R2D^{fl/fl}$ T cells. Moreover, using adoptive T cell transfer in mice xenografted with melanoma, we demonstrated that PPP2R2D deficiency in T cells enhanced the inhibitory effect of Treg cells in anti-tumor immunity. At the translational level, analysis of publicly available data from 418 patients with melanoma revealed that PPP2R2D expression levels correlated positively with tumor-infiltration level of CD4 and CD8 T cells. The data demonstrate that PPP2R2D is a negative regulator of immune checkpoint receptors and its absence exacerbates effector T cell exhaustion and promotes Treg expansion. We conclude that PPP2R2D protects against melanoma growth and PPP2R2D promoting regiments can have therapeutic value in patients with melanoma.

Introduction

The function and numbers of cytotoxic T cells in the tumor microenvironment are critical in the immune-mediated control of cancer (1–3). T cell exhaustion, one of the reasons that T cells lose their effector function, is associated with their inability to exert successful antitumor immune responses (4–6). Programmed cell death 1 protein (PD-1) is well characterized as the dominant inhibitory receptor regulating T cell exhaustion that is upregulated during immune evasion (7). Within the tumor microenvironment, PD-L1, the ligand of PD-1, is expressed on the surface of tumor cells and binds to PD-1 on T cells, which, in turn, suppresses T cell effector functions (6, 8). Blockade of PD-1 that restores

[†]Corresponding author: George C. Tsokos, Beth Israel Deaconess Medical Center, Harvard Medical School, 330 Brookline Ave., CLS-937, Boston, Massachusetts 02215, USA, Phone: 617.735.4160; Fax: 617.735.4170, gtsokos@bidmc.harvard.edu.

T cell cytotoxic capacity *in vivo* has been licensed for use in immunotherapy of several different cancers (9). On the other hand, regulatory T (Treg) cell numbers are increased in the circulation and within tumor sites of various tumor types, which represent another force that mitigates intratumoral effector T cell function (10–12). The intratumoral accumulation of Treg cells has been associated with metastatic disease in several mouse tumor models (13, 14), and, more importantly, with advanced-stage disease and decreased survival in patients with cancer (15). Furthermore, a reduced $CD8^+$ T to Treg cell ratio in the tumor site is predictive of poor clinical outcome (16). Therefore, several approaches have been considered to deplete Treg cells, limit their entry into the tumor tissue and/or disrupt their function (12).

Protein phosphatase 2A (PP2A) is a ubiquitously expressed and highly conserved serine/threonine phosphatase that is important in multiple cellular processes including cell division, cytoskeletal dynamics and various signaling pathways (17). The PP2A core enzyme consists of the scaffold subunit A ($PP2A_A$) and the catalytic subunit C ($PP2A_C$). To form a functional holoenzyme, the core enzyme interacts with one of the many regulatory subunits ($PP2A_B$), which define substrate and tissue specificity (18). Previously, we found that silencing PP2Ac increases IL-2 production in T cells (19), and PP2Ac is requisite for Treg cell function (20) while it enables the expression of IL-17 in T cells (21). In subsequent studies, we showed that PP2A regulatory subunits serve distinct T cell functions with PPP2R2B being responsible for the IL-2 deprivation-induced T cell apoptosis (22), PPP2R2D for limiting IL-2 production and Treg cell function (23) and PPP2R2A for promoting Th1 and Th17 differentiation (24).

Because we previously demonstrated that PPP2R2D deficiency in T cells potentiated the suppressive function of Treg cells and alleviated imiquimod-induced lupus-like pathology (23), we sought to determine the function of PPP2R2D in the control of the anti-tumoral capacity of T cells after we noted in publicly available data that PPP2R2D expression correlated with melanoma tumor growth. In this study, using a melanoma xenograft model, we proved that PPP2R2D deficiency in T cells promotes tumor growth by limiting the number of tumor-infiltrating T cells. Among the infiltrating T cells the effector cells displayed an exhausted phenotype whereas Treg cells were expanded.

Materials and methods

Mice

PPP2R2D flox ($R2D^{fl/fl}$) and $Lck^{cre}R2D^{fl/fl}$ mice were generated using CRISPR/Cas9 technology as described previously (23). Both age- and sex-matched male and female mice at the age of 10–12 weeks (unless indicated otherwise) were used for experiments. All mice were bred and housed in a specific pathogen-free environment in a barrier facility in accordance with the Beth Israel Deaconess Medical Center (BIDMC) Institutional Animal Care and Use Committee (IACUC).

Flow cytometry

Cells were stained with fluorescence-tagged antibodies purchased from eBioscience, BD Pharmingen, or BioLegend (Supplemental Table 1) and analyzed using a Cytoflex flow cytometer. Flow cytometry data were analyzed using CytExpert version 2.0 or Flowjo version 10.6.1. For intracellular cytokine staining, cells were stimulated with 50 ng/mL of phorbol myristate acetate (PMA), 1 μM of ionomycin, and 1 μg/mL of brefeldin A for 4 hours; they were then harvested, fixed, and stained with BD Cytofix/Cytoperm Fixation/ Permeabilization Solution Kit.

Melanoma model

The B16-ova mouse melanoma cells were kindly donated and authenticated by Dr. Cox Terhorst (Division of Immunology at the BIDMC). YUMM1.7 mouse melanoma cells were purchased from ATCC (CRL-3362). The cells were cultured in RPMI medium with 10% fetal bovine serum (FBS) and 1% penicillin/streptomycin (Corning Life Sciences). $R2D^{fl/fl}$ or $Lck^{cre}R2D^{fl/fl}$ mice (8–9 weeks-old) were implanted subcutaneously with B16-ova cells (2×10^5) or YUMM1.7 (3.5×10^5) for 21 days. Tumor sizes were measured using digital caliper. Tumor volume was calculated as $V=Lx\,W^2/2$, where L is the length and W is the width of tumor. At the end of the experiment, spleens, draining lymph nodes and tumors were collected. For tumor infiltration lymphocyte enrichment, tumors were digested with collagenase type IV (300 U/ml, Worthington Biochemical) and DNAse I (100 μg/ml, Roche) in Hank's balanced salt solution (HBSS) for 30 min at 37 °C. The red cells were lysed with ACK lysis buffer for 2 min at room temperature and then cell suspension was loaded onto lymphocyte separation medium (Corning) to enrich lymphocytes. For *ex vivo* stimulation, cells were co-treated with PMA/ionomycin, and brefeldin A (Sigma) for 4 hours and then processed for live/dead, surface, fixation, and intracellular staining.

In vitro inducible (i)Treg cell differentiation

Naive CD4+ T cells were purified using the mouse $CD4^+CD62L^+$ T Cell Isolation Kit II (Miltenyi Biotec). Purified naive T cells were stimulated with plate-bound goat anti-hamster antibodies, soluble anti-CD3 (1 μg/ml,145-2C11; Biolegend) and anti-CD28 (1 μg/ml, 37.51; Biolegend), anti-IL-4 (10 μg/ml) and anti-IFNγ (10 μg/ml) and cytokines such as IL-2 (20 ng/ml; R&D Systems), TGF-β1 (3 ng/ml), for iTreg cells polarization.

Isolation of Tconv cells

Conventional T (Tconv) cells ($Thy1.2^+CD4^+CD25^{lo}CD127^{lo}$ and $Thy1.2^+CD8^+CD25^{lo}CD127^{lo}$) were sorted from freshly isolated mice splenocytes by FACSAria II. Before adoptive T cell transfer, Tconv cells were stimulated with plate-bound goat anti-hamster antibodies, soluble anti-CD3 (1 μg/ml,145-2C11; Biolegend) and anti-CD28 (1 μg/ml, 37.51; Biolegend) for 48 hours.

Adoptive T cell transfer

B16-Ova tumor cells (2×10^5) were injected subcutaneously into Rag1 null ($Rag1^{-/-}$) mice (10-weeks old, Jackson Laboratory) which do not have $CD3^+$ or T cell receptor (TCR) alpha-beta positive cells. On day 6, mice bearing tumors of similar size were divided into

5 groups: receiving no T cells, $R2D^{fl/fl}$ CD4 and CD8 Tconv cells (2×10^6), $Lck^{cre}R2D^{fl/fl}$ CD4 and CD8 Tconv cells (2×10^6), $R2D^{fl/fl}$ CD4 and CD8 Tconv cells (2×10^6) plus $R2D^{fl/fl}$ inducible (i)Treg cells (0.25×10^6), or $Lck^{cre}R2D^{fl/fl}$ CD4 and CD8 Tconv cells (2×10^6) plus $Lck^{cre}R2D^{fl/fl}$ iTreg cells (0.25×10^6). Tumor sizes were measured using digital caliper. Tumor volume was calculated as $V=Lx\,W^2/2$, where L is the length and W is the width of tumor. On day 18, tumors were weighted, digested and analyzed by FACS.

ATAC-seq

ATAC-seq data were obtained from our previously published dataset (GEO accession GSE156927, https://www.ncbi.nlm.nih.gov/geo/query/acc.cgi?acc=GSE156927) (23). The samples for ATAC-seq were from $R2D^{fl/fl}$ and $Lck^{Cre}R2D^{fl/fl}$ $CD4^+$ T conventional (Tconv) cells ($Thy1.2^+CD4^+CD25^{lo}CD127^{lo}$) which were sorted out by flow cytometry and stimulated with plate-bound CD3 (1 μg/mL) and CD28 (1 μg/mL) antibodies for 4 hours. Analysis of ATAC-seq data was previously described (23).

Statistics

All statistical analyses were conducted using GraphPad Prism 7 (GraphPad software Inc.). Data were presented as mean ± SD unless indicated otherwise in the figure legend. Statistical differences between 2 populations were calculated by t test (2-tailed) including multiple t test, or unpaired t test. For multiple populations' comparison, 2-way ANOVA with Holm-Šidák multiple-comparisons test was used. $P < 0.05$ was considered statistically significant.

Study approval

All animal procedures were approved by the IACUC of BIDMC, Harvard Medical School. All mice were maintained in a specific pathogen free animal facility (BIDMC). All mice were genotyped to validate claimed strain.

Results

PPP2R2D deficiency in T cells reduces the percentage of central and effector memory T cells and alters cytokine production

We had previously shown that PPP2R2D deficiency in T cells does not impair T cell development in the thymus and T cell subset distribution in the spleen (23). However, the percentage of central/effector memory cells among $CD4^+$ and $CD8^+$ T cell populations ($CD62L^+CD44^+$ and $CD62L^-CD44^+$) in the spleens were significantly decreased in $Lck^{Cre}R2D^{fl/fl}$ compared to their $R2D^{fl/fl}$ littermates (Figure 1A). When stimulated *ex vivo* with phorbol myristate acetate (PMA) and ionomycin for 4 hours, both $CD4^+$ and $CD8^+$ T cells from $Lck^{Cre}R2D^{fl/fl}$ mice displayed significantly fewer percentages of interferon-γ (IFN-γ)-producing cells (Figure 1B), but larger proportions of interleukin-2 (IL-2)-producing cells (Figure 1C) compared to cells from their $R2D^{fl/fl}$ counterparts. Yet, the regulatory T (Treg) cell subset ($CD3^+CD4^+Foxp3^+CD25^{hi}$) in the spleens was comparable between $R2D^{fl/fl}$ and $Lck^{Cre}R2D^{fl/fl}$ mice (Figure 1D). These data are in line with our previously published results which showed that PPP2R2D-deficient Treg cells were

more efficient than wild type Treg cells in suppressing the IFN-γ expression of $CD4^+$ or $CD8^+$ T cells (23).

PPP2R2D deficiency in T cells promotes melanoma growth in mice by decreasing the numbers of tumor-infiltrating T cells

To further examine the function of PPP2R2D-deficient T cells *in vivo* in the context of tumor immunity, we injected mouse melanoma B16-Ova (2×10^5) or YUMM1.7 (3.5×10^5) cells subcutaneously into $R2D^{fl/fl}$ and $Lck^{cre}R2D^{fl/fl}$ mice. As shown in Figures 2A and 2B, and Supplemental Figures 1A and 1B, tumors grew faster in $Lck^{cre}R2D^{fl/fl}$ mice and showed increased size and weight compared to those developing in $R2D^{fl/fl}$ mice. On day 21 after injection of melanoma cells, mice were euthanized to collect spleens, draining lymph nodes (dLNs) and tumors and lymphocytes were isolated, counted and analyzed by FACS staining. Importantly, the percentage and numbers of $CD3^+$ T cells (Figures 3A and 3B; Supplemental Figures 1C and 1D) in the tumors harvested from $Lck^{cre}R2D^{fl/fl}$ mice were significantly decreased compared to those from $R2D^{fl/fl}$ mice. Both the numbers of $CD4^+$ and $CD8^+$ T cell subsets were decreased among the tumor infiltrating lymphocytes (TILs) (Figure 3C; Supplemental Figure 1E). Although there was no significant difference in the proportions of $CD3^+$ T cells (Figures 3D and 3E; Supplemental Figures 1F and 1G), the numbers of $CD3^+$, $CD4^+$ and $CD8^+$ T cells in the dLNs isolated from $Lck^{cre}R2D^{fl/fl}$ mice were significantly reduced when compared with those from $R2D^{fl/fl}$ mice (Figure 3F; Supplemental Figure 1H). Yet, the proportions and numbers of $CD3^+$, $CD3^+CD4^+$ and $CD3^+CD8^+$ T cells were comparable in the spleens of $R2D^{fl/fl}$ and $Lck^{cre}R2D^{fl/fl}$ mice (Figures 3G–3I; Supplemental Figures 1I–1K). We further analyzed TCGA RNA sequencing (RNA-seq) data from 418 patients with melanoma from the Tumor Immune Estimation Resource (TIMER) (25) to examine the possible relevance of the PPP2R2D expression and immune cell infiltration in human melanoma. Consistent with the findings in mice, PPP2R2D expression levels in the tumor-infiltrating immune cells correlated positively with the infiltration levels of $CD8^+$ ($P = 0.00000769$) and $CD4^+$ T cells ($P = 0.00172$) but not with B cells ($P = 0.288$) (Figure 3J). Collectively, these data suggest that PPP2R2D deficiency in T cells promotes melanoma tumor growth by decreasing the infiltration of T cells into tumors.

PPP2R2D deficiency in T cells increases T cell exhaustion of tumor-infiltrating T cells.

Our aforementioned findings that the numbers of $CD3^+$, $CD3^+CD4^+$ and $CD3^+CD8^+$ T cells in dLNs and TILs were significantly decreased in $Lck^{cre}R2D^{fl/fl}$ mice as compared to $R2D^{fl/fl}$ mice (Figures 3C and 3F; Supplemental Figures 1E and 1H) raised the question of whether their effector functions were also affected. Interestingly, the proportions of both $CD4^+$ (Figures 4A and 4B; Supplemental Figure 1L) and $CD8^+$ (Figures 4C and 4D; Supplemental Figure 1M) central/effector memory T cell populations ($CD62L^+CD44^+$ and $CD62L^-CD44^+$) were decreased in the dLNs and TILs of $Lck^{Cre}R2D^{fl/fl}$ compared to those of $R2D^{fl/fl}$ mice. T cell exhaustion is associated with effector T cell function and the inability to mount successful antitumor immune response (4–6). The inhibitory receptor PD-1 has been well characterized as an exhaustion marker of T cells and controls the magnitude of T cell effector functions upon activation (7). The percentage of PD-1-expressing cells ($CD3^+CD44^+PD\text{-}1^+$) of the effector T cells ($CD3^+CD44^+$) in TILs from $Lck^{Cre}R2D^{fl/fl}$ mice were increased when compared to those from $R2D^{fl/fl}$ mice (Figures

4E and 4F; Supplemental Figure 1N) as they were in both $CD4^+$ and $CD8^+$ subsets. Because IFN-γ is important in T cell function in tumor immunity (26), we considered the production of IFN-γ by T cells and found that the percentages of $CD3^+CD4^+$IFN-γ^+ and $CD3^+CD8^+$ IFN-γ^+-producing T cells were significantly decreased in tumors from $Lck^{cre}R2D^{fl/fl}$ compared to $R2D^{fl/fl}$ mice (Figures 4G and 4H; Supplemental Figure 1O). These results indicate that PPP2R2D deficiency in T cells increased T cell exhaustion of tumor-infiltrating T cells. To further confirm the role of PPP2R2D in the regulation of T cell exhaustion, we analyzed our previously published ATAC-seq dataset (GEO accession: GSE156927) (23) obtained from $CD4^+$ Tconv cells that had been sorted by flow cytometry from spleens of $R2D^{fl/fl}$ or $Lck^{Cre}R2D^{fl/fl}$ mice and stimulated *in vitro* by plate-bound CD3 and CD28 antibodies for 4 hours. As presented in Figure 4I, sequencing read densities at genes encoding known T cell exhaustion markers such as *PDCD1* (PD-1), *LAG3*, *HAVCR2* (Tim3) and *CTLA4* were increased in $Lck^{Cre}R2D^{fl/fl}$ Tconv cells compared with those in $R2D^{fl/fl}$ Tconv cells, demonstrating that lack of PPP2R2D expression promoted chromatin accessibility to genes involved in T cell exhaustion.

PPP2R2D deficiency in T cells increases Treg population in tumor-infiltrating T cells.

In tumor immunity, Treg cells are involved in tumor development and progression by inhibiting antitumor immunity (12). As shown in Figures 5A and 5B, and Supplemental Figures 2A and 2B, the percentage of Treg cells ($CD3^+CD4^+FoxP3^+CD25^{hi}$) was significantly increased in tumors but not in the spleens and dLNs of $Lck^{cre}R2D^{fl/fl}$ compared to $R2D^{fl/fl}$ mice. Moreover, a dramatic reduction of $CD3^+CD8^+$ to Treg cell ratio (Figure 5C; Supplemental Figure 2C) was observed in TILs of $Lck^{cre}R2D^{fl/fl}$ compared to $R2D^{fl/fl}$ mice. In addition, we found that the percentages of IL-2-producing $CD4^+$ and $CD8^+$ T cells were increased in the spleens, dLNs, and tumors from $Lck^{cre}R2D^{fl/fl}$ compared to those in $R2D^{fl/fl}$ mice (Figures 5D and 5E; Supplemental Figures 2D and 2E). These data imply that PPP2R2D deficiency in T cells increases Treg population in tumor-infiltrating T cells probably because of the increase in the percentage of IL-2-producing $Lck^{Cre}R2D^{fl/fl}$ T cells.

PPP2R2D deficiency in T cells enhanced the inhibitory effect of Treg cells on anti-tumor immunity.

In order to characterize whether the Treg population in tumor-infiltrating T cells contributes to the inhibition of the anti-tumor immunity, we assessed the ability of $R2D^{fl/fl}$ or $Lck^{cre}R2D^{fl/fl}$ Treg cells to inhibit the efficacy of adoptively transferred T cells. B16-Ova tumor cells (2×10^5) were injected subcutaneously into Rag1 null (*$Rag1^{-/-}$*) mice which do not have $CD3^+$ or T cell receptor (TCR) alpha-beta positive cells. On day 6, mice bearing tumors of similar size were divided into 5 groups receiving: no T cells, $R2D^{fl/fl}$ CD4 and CD8 conventional T (Tconv) cells (2×10^6), $Lck^{cre}R2D^{fl/fl}$ CD4 and CD8 Tconv cells (2×10^6), $R2D^{fl/fl}$ CD4 and CD8 Tconv cells (2×10^6) plus $R2D^{fl/fl}$ inducible (i)Treg cells (0.25×10^6), or $Lck^{cre}R2D^{fl/fl}$ CD4 and CD8 Tconv cells (2×10^6) plus $Lck^{cre}R2D^{fl/fl}$ iTreg cells (0.25×10^6). As shown in Figures 6A and 6B, $Lck^{cre}R2D^{fl/fl}$ Tconv cells exerted enhanced anti-tumor activity as compared to $R2D^{fl/fl}$ Tconv cells, which is consistent with published data (27). Moreover, both $R2D^{fl/fl}$ and $Lck^{cre}R2D^{fl/fl}$ Treg cells significantly inhibited the anti-tumor activity of $R2D^{fl/fl}$ and $Lck^{cre}R2D^{fl/fl}$ Tconv cells (Figures 6A and 6B), respectively. Importantly, $Lck^{cre}R2D^{fl/fl}$ Treg cells displayed an enhanced inhibitory

effect on $Lck^{cre}R2D^{fl/fl}$ Tconv cells as compared to the inhibitory effect of $R2D^{fl/fl}$ Treg cells on $R2D^{fl/fl}$ Tconv cells (Figures 6A and 6B). Interestingly, a dramatic reduction of $CD4^+$ and $CD8^+$ T cell to Treg cell ratio (Figure 6C) was observed in TILs of $Lck^{cre}R2D^{fl/fl}$ Tconv plus $Lck^{cre}R2D^{fl/fl}$ Treg cell compared to $R2D^{fl/fl}$ Tconv plus $R2D^{fl/fl}$ Treg cell groups. These results suggest that PPP2R2D deficiency in T cells enhances the inhibitory effect of Treg cells in anti-tumor immunity.

Discussion

In this communication, we present evidence that PPP2R2D deficiency in T cells promotes melanoma growth in mice by decreasing the number of tumor-infiltrating T cells. Mechanistically, PPP2R2D limits T cell exhaustion by controlling chromatin accessibility of immune checkpoint inhibitory receptors including PD-1, LAG3, TIM3 and CTLA4, and promotes the expansion of Treg cells in tumor-infiltrating T cells probably because of increased IL-2 production. Our report introduces PPP2R2D as a negative regulator of immune checkpoint control mechanisms and Treg expansion in melanoma.

The global incidence of melanoma continues to rise, and the mortality associated with unresectable or metastatic melanoma remains high. T cell exhaustion, which is associated with attenuated cytotoxic capacity of effector T cells, contributes to the failure of antitumor immune responses (4–6). PD-1 and CTLA4 are the most notable immune checkpoint inhibitory receptors that are expressed on the surface of the effector T cells and exacerbate their exhaustion (6, 7). During the past decade, although progress in the treatment of advanced melanoma using immune checkpoint (PD-1 or CTLA4) blocking antibodies has markedly improved survival outcomes (28–32), the proportion of response (10%–30%) (28, 32, 33) and long-term survival rates (~ 20%) (32, 34, 35) in treated patients remain low. Thus, further understanding of the regulation of immune checkpoints may help improve the therapeutic strategies. In this report, we identify that, under T cell receptor (TCR) stimulation, PPP2R2D negatively controls the chromatin opening of T cell exhaustion markers such as PD-1, LAG3, TIM3 and CTLA4, implying that PPP2R2D is a regulator of multiple immune checkpoint inhibitory receptors. This information could be beneficial for designing drugs targeting multiple immune checkpoint inhibitory receptors, since the clinical benefit is enhanced by the co-administration of antibodies targeting CTLA-4 and PD-1 in patients with advanced melanoma when compared to monotherapy (29).

We observed an expansion of PD-1-expressing cell subset of central/effector memory T cells ($CD3^+CD4^+CD44^+PD\text{-}1^+$ and $CD3^+CD8^+CD44^+PD\text{-}1^+$) in PPP2R2D-deficient compared to wild-type T cells in TILs, suggesting that PPP2R2D-deficient effector T cells are more exhausted within the tumor microenvironment. In the tumor milieu, PD-L1, the ligand of PD-1, is expressed on the surface of tumor cells and binds to PD-1 on T cells, which, in turn, suppresses T cell effector functions (6, 7). This claim is in agreement with our observation that fewer IFN-γ-producing T cells resided in tumors from $Lck^{cre}R2D^{fl/fl}$ compared to $R2D^{fl/fl}$ mice. Moreover, we obtained fewer numbers of tumor-infiltrating T cells in $Lck^{cre}R2D^{fl/fl}$ mice probably because PD-L1 promotes T cell apoptosis when it binds to PD-1 expressed on the T cells (8). Tumors often take advantage of these negative feedback mechanisms to create an overall immunosuppressive state and escape

immunosurveillance of cancer (1–3). Indeed, as presented in this study, the tumors that grew in $Lck^{Cre}R2D^{fl/fl}$ mice had bigger size than in $R2D^{fl/fl}$ mice.

Treg cells limit the antitumor immune response and promote angiogenesis and tumor growth. Their immunosuppressive function may, in part, explain the failure of many immunotherapies in cancer (12). Indeed Treg cell numbers are increased in the circulation and within tumors of various origins (10–12). We previously demonstrated that PPP2R2D deficiency up-regulates IL-2 production by conventional T cells (23). IL-2 administration increases Treg cells in patients with cancer (36–38) which is in line with our findings of increased percentages of Treg cells and decreased ratio of $CD8^+$/Treg cells in tumors of mice with PPP2R2D-deficient T cells. The intratumoral accumulation of Treg cells has been associated with tumor progression (13, 14) and with advanced-stage disease and decreased survival in patients with cancer (15). In agreement, we observed bigger tumors to grow in $Lck^{Cre}R2D^{fl/fl}$ mice. Interestingly, this result contradicts the finding by Zhou et al (27) that adoptive transfer of *in vitro* activated $CD4^+$ and $CD8^+$ T cells in which PPP2R2D had been silenced using shRNA technology into mice bearing melanoma enhanced the anti-tumor immunity. The contradictory effect is most probably due to the fact that Zhou et al transferred activated PPP2R2D-insufficient $CD4^+$ and $CD8^+$ T cells into mice 12 days after the melanoma cells had been inoculated (27), whereas in our model, PPP2R2D-deficient T cells producing more IL-2, which promoted Treg expansion, had been present at the time of the injection of melanoma cells. Treg cells highly express CTLA-4 that inhibits an immune response by attenuating T cell activation at a proximal step in the immune response (39). Consistent with this, we proved in this study that PPP2R2D deficiency in T cells reduced the proportion of central/effector memory T cells ($CD3^+CD44^+$) in the TILs, $Lck^{cre}R2D^{fl/fl}$ Treg cells displayed enhanced inhibitory effect on $Lck^{cre}R2D^{fl/fl}$ Tconv cells as compared to the inhibitory effect of $R2D^{fl/fl}$ Treg cells on $R2D^{fl/fl}$ Tconv cells and in our previous study (23) that PPP2R2D-deficient Treg cells displayed a more suppressive effect on the expression of IFN-γ and proliferation of $CD4^+$ or $CD8^+$ T cells following stimulation *in vitro*.

In summary, we have shown that PPP2R2D is a negative regulator of immune checkpoint inhibitory receptors and its absence exacerbates effector T cell exhaustion and promotes Treg expansion. Our findings have significant translational value because in patients with melanoma PPP2R2D expression levels in the tumor-infiltrating T cells correlate positively with the intensity of infiltration of $CD8^+$ and $CD4^+$ T cells.

Supplementary Material

Refer to Web version on PubMed Central for supplementary material.

Acknowledgments

Work was supported by NIH grant RO1 AI136924. MS is supported by the Société Française de Rhumatologie, Arthur-Sachs & Monahan fellowships and Philippe Foundation.

References:

1. Galon J, Costes A, Sanchez-Cabo F, Kirilovsky A, Mlecnik B, Lagorce-Pages C, Tosolini M, Camus M, Berger A, Wind P, Zinzindohoue F, Bruneval P, Cugnenc PH, Trajanoski Z, Fridman WH, and

Pages F. 2006. Type, density, and location of immune cells within human colorectal tumors predict clinical outcome. Science 313: 1960–1964. [PubMed: 17008531]

2. Mahmoud SM, Paish EC, Powe DG, Macmillan RD, Grainge MJ, Lee AH, Ellis IO, and Green AR. 2011. Tumor-infiltrating CD8+ lymphocytes predict clinical outcome in breast cancer. J Clin Oncol 29: 1949–1955. [PubMed: 21483002]
3. Oble DA, Loewe R, Yu P, and Mihm MC Jr. 2009. Focus on TILs: prognostic significance of tumor infiltrating lymphocytes in human melanoma. Cancer Immun 9: 3. [PubMed: 19338264]
4. McLane LM, Abdel-Hakeem MS, and Wherry EJ. 2019. CD8 T Cell Exhaustion During Chronic Viral Infection and Cancer. Annu Rev Immunol 37: 457–495. [PubMed: 30676822]
5. Sharma P, and Allison JP. 2015. The future of immune checkpoint therapy. Science 348: 56–61. [PubMed: 25838373]
6. Wherry EJ 2011. T cell exhaustion. Nat Immunol 12: 492–499. [PubMed: 21739672]
7. Boussiotis VA 2016. Molecular and Biochemical Aspects of the PD-1 Checkpoint Pathway. N Engl J Med 375: 1767–1778. [PubMed: 27806234]
8. Dong H, Strome SE, Salomao DR, Tamura H, Hirano F, Flies DB, Roche PC, Lu J, Zhu G, Tamada K, Lennon VA, Celis E, and Chen L. 2002. Tumor-associated B7-H1 promotes T-cell apoptosis: a potential mechanism of immune evasion. Nat Med 8: 793–800. [PubMed: 12091876]
9. Hargadon KM, Johnson CE, and Williams CJ. 2018. Immune checkpoint blockade therapy for cancer: An overview of FDA-approved immune checkpoint inhibitors. Int Immunopharmacol 62: 29–39. [PubMed: 29990692]
10. Facciabene A, Motz GT, and Coukos G. 2012. T-regulatory cells: key players in tumor immune escape and angiogenesis. Cancer Res 72: 2162–2171. [PubMed: 22549946]
11. Facciabene A, Peng X, Hagemann IS, Balint K, Barchetti A, Wang LP, Gimotty PA, Gilks CB, Lal P, Zhang L, and Coukos G. 2011. Tumour hypoxia promotes tolerance and angiogenesis via CCL28 and T(reg) cells. Nature 475: 226–230. [PubMed: 21753853]
12. Sharabi A, Tsokos MG, Ding Y, Malek TR, Klatzmann D, and Tsokos GC. 2018. Regulatory T cells in the treatment of disease. Nat Rev Drug Discov 17: 823–844. [PubMed: 30310234]
13. Halvorsen EC, Mahmoud SM, and Bennewith KL. 2014. Emerging roles of regulatory T cells in tumour progression and metastasis. Cancer Metastasis Rev 33: 1025–1041. [PubMed: 25359584]
14. Facciabene A, Santoro S, and Coukos G. 2012. Know thy enemy: Why are tumor-infiltrating regulatory T cells so deleterious? Oncoimmunology 1: 575–577. [PubMed: 22754792]
15. Shang B, Liu Y, and Jiang SJ. 2015. Prognostic value of tumor-infiltrating FoxP3+ regulatory T cells in cancers: a systematic review and meta-analysis. Sci Rep 5: 15179. [PubMed: 26462617]
16. Bates GJ, Fox SB, Han C, Leek RD, Garcia JF, Harris AL, and Banham AH. 2006. Quantification of regulatory T cells enables the identification of high-risk breast cancer patients and those at risk of late relapse. J Clin Oncol 24: 5373–5380. [PubMed: 17135638]
17. Ruvolo PP 2016. The broken “Off” switch in cancer signaling: PP2A as a regulator of tumorigenesis, drug resistance, and immune surveillance. BBA Clin 6: 87–99. [PubMed: 27556014]
18. Shi Y 2009. Serine/threonine phosphatases: mechanism through structure. Cell 139: 468–484. [PubMed: 19879837]
19. Katsiari CG, Kyttaris VC, Juang YT, and Tsokos GC. 2005. Protein phosphatase 2A is a negative regulator of IL-2 production in patients with systemic lupus erythematosus. J Clin Invest 115: 3193–3204. [PubMed: 16224536]
20. Apostolidis SA, Rodriguez-Rodriguez N, Suarez-Fueyo A, Dioufa N, Ozcan E, Crispin JC, Tsokos MG, and Tsokos GC. 2016. Phosphatase PP2A is requisite for the function of regulatory T cells. Nat Immunol 17: 556–564. [PubMed: 26974206]
21. Apostolidis SA, Rauen T, Hedrich CM, Tsokos GC, and Crispin JC. 2013. Protein phosphatase 2A enables expression of interleukin 17 (IL-17) through chromatin remodeling. J Biol Chem 288: 26775–26784. [PubMed: 23918926]
22. Crispin JC, Apostolidis SA, Finnell MI, and Tsokos GC. 2011. Induction of PP2A Bbeta, a regulator of IL-2 deprivation-induced T-cell apoptosis, is deficient in systemic lupus erythematosus. Proc Natl Acad Sci U S A 108: 12443–12448. [PubMed: 21746932]

23. Pan W, Sharabi A, Ferretti A, Zhang Y, Burbano C, Yoshida N, Tsokos MG, and Tsokos GC. 2020. PPP2R2D suppresses IL-2 production and Treg function. JCI Insight 5.
24. Pan W, Nagpal K, Suarez-Fueyo A, Ferretti A, Yoshida N, Tsokos MG, and Tsokos GC. 2021. The Regulatory Subunit PPP2R2A of PP2A Enhances Th1 and Th17 Differentiation through Activation of the GEF-H1/RhoA/ROCK Signaling Pathway. J Immunol 206: 1719–1728. [PubMed: 33762326]
25. Li B, Severson E, Pignon JC, Zhao H, Li T, Novak J, Jiang P, Shen H, Aster JC, Rodig S, Signoretti S, Liu JS, and Liu XS. 2016. Comprehensive analyses of tumor immunity: implications for cancer immunotherapy. Genome Biol 17: 174. [PubMed: 27549193]
26. Nakajima C, Uekusa Y, Iwasaki M, Yamaguchi N, Mukai T, Gao P, Tomura M, Ono S, Tsujimura T, Fujiwara H, and Hamaoka T. 2001. A role of interferon-gamma (IFN-gamma) in tumor immunity: T cells with the capacity to reject tumor cells are generated but fail to migrate to tumor sites in IFN-gamma-deficient mice. Cancer Res 61: 3399–3405. [PubMed: 11309299]
27. Zhou P, Shaffer DR, Alvarez Arias DA, Nakazaki Y, Pos W, Torres AJ, Cremasco V, Dougan SK, Cowley GS, Elpek K, Brogdon J, Lamb J, Turley SJ, Ploegh HL, Root DE, Love JC, Dranoff G, Hacohen N, Cantor H, and Wucherpfennig KW. 2014. In vivo discovery of immunotherapy targets in the tumour microenvironment. Nature 506: 52–57. [PubMed: 24476824]
28. Hodi FS, O'Day SJ, McDermott DF, Weber RW, Sosman JA, Haanen JB, Gonzalez R, Robert C, Schadendorf D, Hassel JC, Akerley W, van den Eertwegh AJ, Lutzky J, Lorigan P, Vaubel JM, Linette GP, Hogg D, Ottensmeier CH, Lebbe C, Peschel C, Quirt I, Clark JI, Wolchok JD, Weber JS, Tian J, Yellin MJ, Nichol GM, Hoos A, and Urba WJ. 2010. Improved survival with ipilimumab in patients with metastatic melanoma. N Engl J Med 363: 711–723. [PubMed: 20525992]
29. Larkin J, Chiarion-Sileni V, Gonzalez R, Grob JJ, Rutkowski P, Lao CD, Cowey CL, Schadendorf D, Wagstaff J, Dummer R, Ferrucci PF, Smylie M, Hogg D, Hill A, Marquez-Rodas I, Haanen J, Guidoboni M, Maio M, Schoffski P, Carlino MS, Lebbe C, McArthur G, Ascierto PA, Daniels GA, Long GV, Bastholt L, Rizzo JI, Balogh A, Moshyk A, Hodi FS, and Wolchok JD. 2019. Five-Year Survival with Combined Nivolumab and Ipilimumab in Advanced Melanoma. N Engl J Med 381: 1535–1546. [PubMed: 31562797]
30. Valsecchi ME 2015. Combined Nivolumab and Ipilimumab or Monotherapy in Untreated Melanoma. N Engl J Med 373: 1270.
31. Eggermont AMM, Blank CU, Mandala M, Long GV, Atkinson V, Dalle S, Haydon A, Lichinitser M, Khattak A, Carlino MS, Sandhu S, Larkin J, Puig S, Ascierto PA, Rutkowski P, Schadendorf D, Koornstra R, Hernandez-Aya L, Maio M, van den Eertwegh AJM, Grob JJ, Gutzmer R, Jamal R, Lorigan P, Ibrahim N, Marreaud S, van Akkooi ACJ, Suciu S, and Robert C. 2018. Adjuvant Pembrolizumab versus Placebo in Resected Stage III Melanoma. N Engl J Med 378: 1789–1801. [PubMed: 29658430]
32. Robert C, Long GV, Brady B, Dutriaux C, Maio M, Mortier L, Hassel JC, Rutkowski P, McNeil C, Kalinka-Warzocha E, Savage KJ, Hernberg MM, Lebbe C, Charles J, Mihalcioiu C, Chiarion-Sileni V, Mauch C, Cognetti F, Arance A, Schmidt H, Schadendorf D, Gogas H, Lundgren-Eriksson L, Horak C, Sharkey B, Waxman IM, Atkinson V, and Ascierto PA. 2015. Nivolumab in previously untreated melanoma without BRAF mutation. N Engl J Med 372: 320–330. [PubMed: 25399552]
33. Robert C, Thomas L, Bondarenko I, O'Day S, Weber J, Garbe C, Lebbe C, Baurain JF, Testori A, Grob JJ, Davidson N, Richards J, Maio M, Hauschild A, Miller WH Jr., Gascon P, Lotem M, Harmankaya K, Ibrahim R, Francis S, Chen TT, Humphrey R, Hoos A, and Wolchok JD. 2011. Ipilimumab plus dacarbazine for previously untreated metastatic melanoma. N Engl J Med 364: 2517–2526. [PubMed: 21639810]
34. Maio M, Grob JJ, Aamdal S, Bondarenko I, Robert C, Thomas L, Garbe C, Chiarion-Sileni V, Testori A, Chen TT, Tschaika M, and Wolchok JD. 2015. Five-year survival rates for treatment-naive patients with advanced melanoma who received ipilimumab plus dacarbazine in a phase III trial. J Clin Oncol 33: 1191–1196. [PubMed: 25713437]
35. Schadendorf D, Hodi FS, Robert C, Weber JS, Margolin K, Hamid O, Patt D, Chen TT, Berman DM, and Wolchok JD. 2015. Pooled Analysis of Long-Term Survival Data From Phase II and

Phase III Trials of Ipilimumab in Unresectable or Metastatic Melanoma. J Clin Oncol 33: 1889–1894. [PubMed: 25667295]

36. Ahmadzadeh M, and Rosenberg SA. 2006. IL-2 administration increases CD4+ CD25(hi) Foxp3+ regulatory T cells in cancer patients. Blood 107: 2409–2414. [PubMed: 16304057]
37. Jensen HK, Donskov F, Nordsmark M, Marcussen N, and von der Maase H. 2009. Increased intratumoral FOXP3-positive regulatory immune cells during interleukin-2 treatment in metastatic renal cell carcinoma. Clin Cancer Res 15: 1052–1058. [PubMed: 19188179]
38. Sim GC, Martin-Orozco N, Jin L, Yang Y, Wu S, Washington E, Sanders D, Lacey C, Wang Y, Vence L, Hwu P, and Radvanyi L. 2014. IL-2 therapy promotes suppressive ICOS+ Treg expansion in melanoma patients. J Clin Invest 124: 99–110. [PubMed: 24292706]
39. Krummel MF, and Allison JP. 1996. CTLA-4 engagement inhibits IL-2 accumulation and cell cycle progression upon activation of resting T cells. J Exp Med 183: 2533–2540. [PubMed: 8676074]

Key points:

- PPP2R2D limits T cell exhaustion by controlling chromatin accessibility
- PPP2R2D deficiency in T cells promotes tumor growth of melanoma
- PPP2R2D deficiency in T cells expands Treg population in tumor-infiltrating T cells

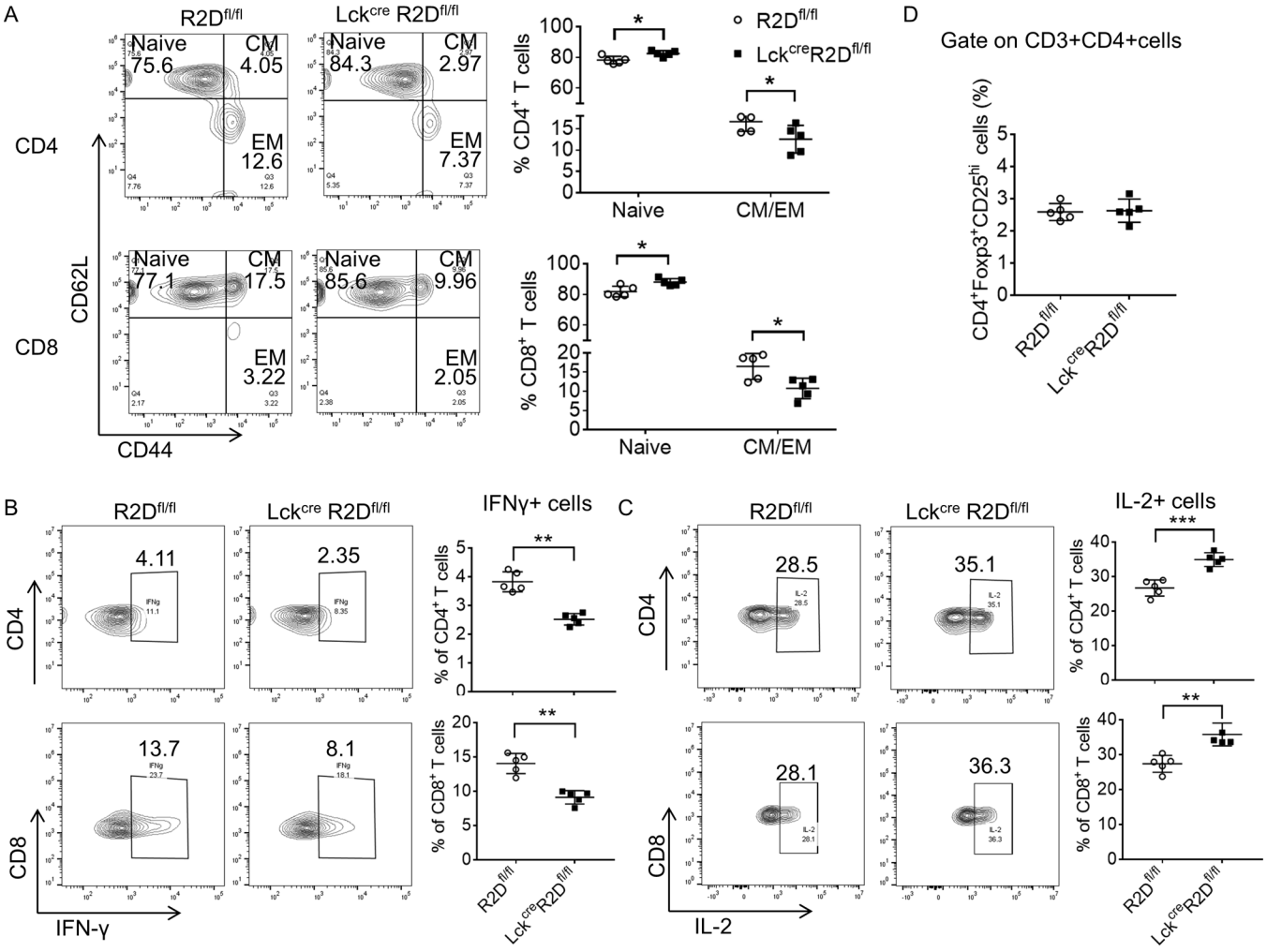

Figure 1. PPP2R2D deficiency in T cells reduces central and effector memory T cells and alters cytokines production.

(**A**) Splenocytes isolated from $R2D^{fl/fl}$ and $Lck^{Cre}R2D^{fl/fl}$ mice were stained with CD3, CD4, CD8, CD62L and CD44 antibodies and analyzed by flow cytometry. **Left**: Representative flow cytometry plots. **Right**: Cumulative data (n = 5 mice/group) depicting the percentages of splenic naïve ($CD62L^{+}CD44^{-}$) and central/effector memory (CM/EM; $CD62L^{+}CD44^{+}$, $CD62L^{-}CD44^{+}$) subsets. **(B-C)** Splenocytes isolated from $R2D^{fl/fl}$ and $Lck^{Cre}R2D^{fl/fl}$ mice stimulated *ex vivo* with phorbol myristate acetate (PMA) and ionomycin for 4 hours before FACS analysis. Representative flow cytometry plots are shown (**B and C, left**). Cumulative data (*n* = 5 mice/group) depicting the percentages of IFN-γ- (**B, right**) and IL-2- (**C, right**) positive cells. (**D**) Treg cell subset ($CD4^{+}Foxp3^{+}CD25^{hi}$) as a percentage of $CD3^{+}CD4^{+}$ T cells in the spleen of $R2D^{fl/fl}$ and $Lck^{Cre}R2D^{fl/fl}$ mice (*n* = 5 mice/group). All the data were obtained from two independent experiments. **P<0.05, **P<0.01 and ***P<0.001* by unpaired *T* test.

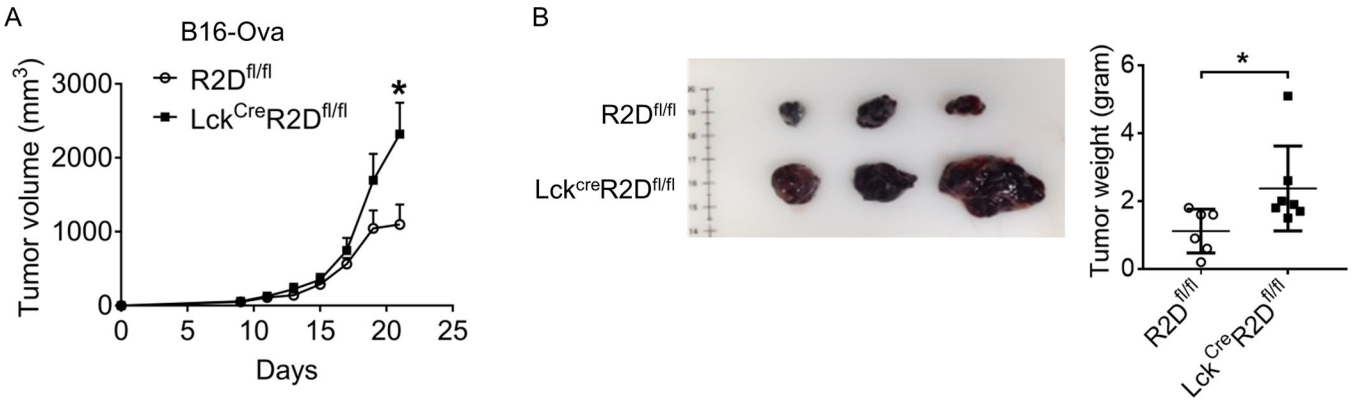

Figure 2. PPP2R2D deficiency in T cells promotes B16-ova melanoma tumor growth in mice.

B16-ova melanoma cells (2×10^5) were subcutaneously injected into $R2D^{fl/fl}$ (n = 6) or $Lck^{cre}R2D^{fl/fl}$ (n = 7) mice and monitored for 21 days. (**A**) Tumor size was monitored every other day by measuring 3 diameters using digital caliper until day 21. (**B**) On day 21, mice were euthanized and tumors were collected. **Left**: pictures of tumors harvested from $R2D^{fl/fl}$ or $Lck^{cre}R2D^{fl/fl}$ mice. **Right**: tumor weight. All the data were obtained from two independent experiments. *$P<0.05$* by two-way ANOVA with Holm-Šidákmultiple-comparisons test (**A**) or by unpaired *T* test (**B**).

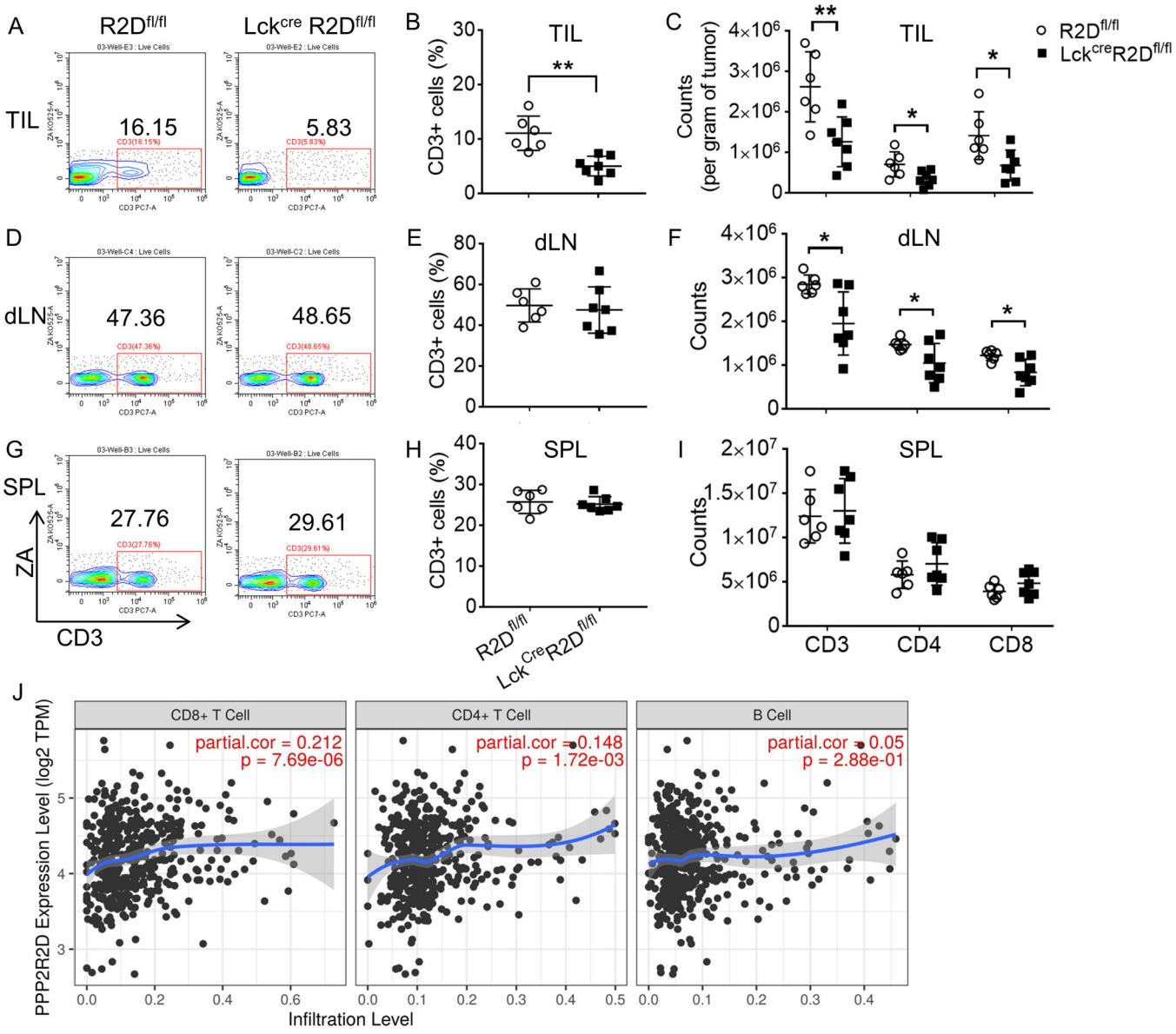

Figure 3. PPP2R2D deficiency in T cells decreases the percentage and numbers of tumor-infiltrating T cells.

(**A-I**) B16-ova melanoma cells (2×10^5) were subcutaneously injected into $R2D^{fl/fl}$ (n = 6) or $Lck^{cre}R2D^{fl/fl}$ (n = 7) mice. On day 21 after injection of melanoma cells, mice were euthanized to collect tumors (**TIL**), draining lymph nodes (**dLN**), and spleens (**SPL**), and the lymphocytes were isolated, counted and analyzed by FACS staining. Representative flow cytometry plots (**A, D and G**) and cumulative data (**B, E and H**) showing $CD3^+$ cells as the percentage of lymphocytes in the TIL (**A and B**), dLN (**D and E**) or SPL (**G and H**). Absolute numbers of CD3+, $CD3^+CD4^+$, and $CD3^+CD8^+$ cells in the TIL (**C**), dLN (**F**) and SPL (**I**). All the data were obtained from two independent experiments. **P<0.05,* and ***P<0.01* by unpaired *T* test. (**J**) TCGA RNA sequencing (RNA-seq) data from 418 patients with melanoma obtained from the Tumor Immune Estimation Resource (TIMER)

were analyzed and the relevance of the PPP2R2D expression and immune cell infiltration in human melanoma is shown.

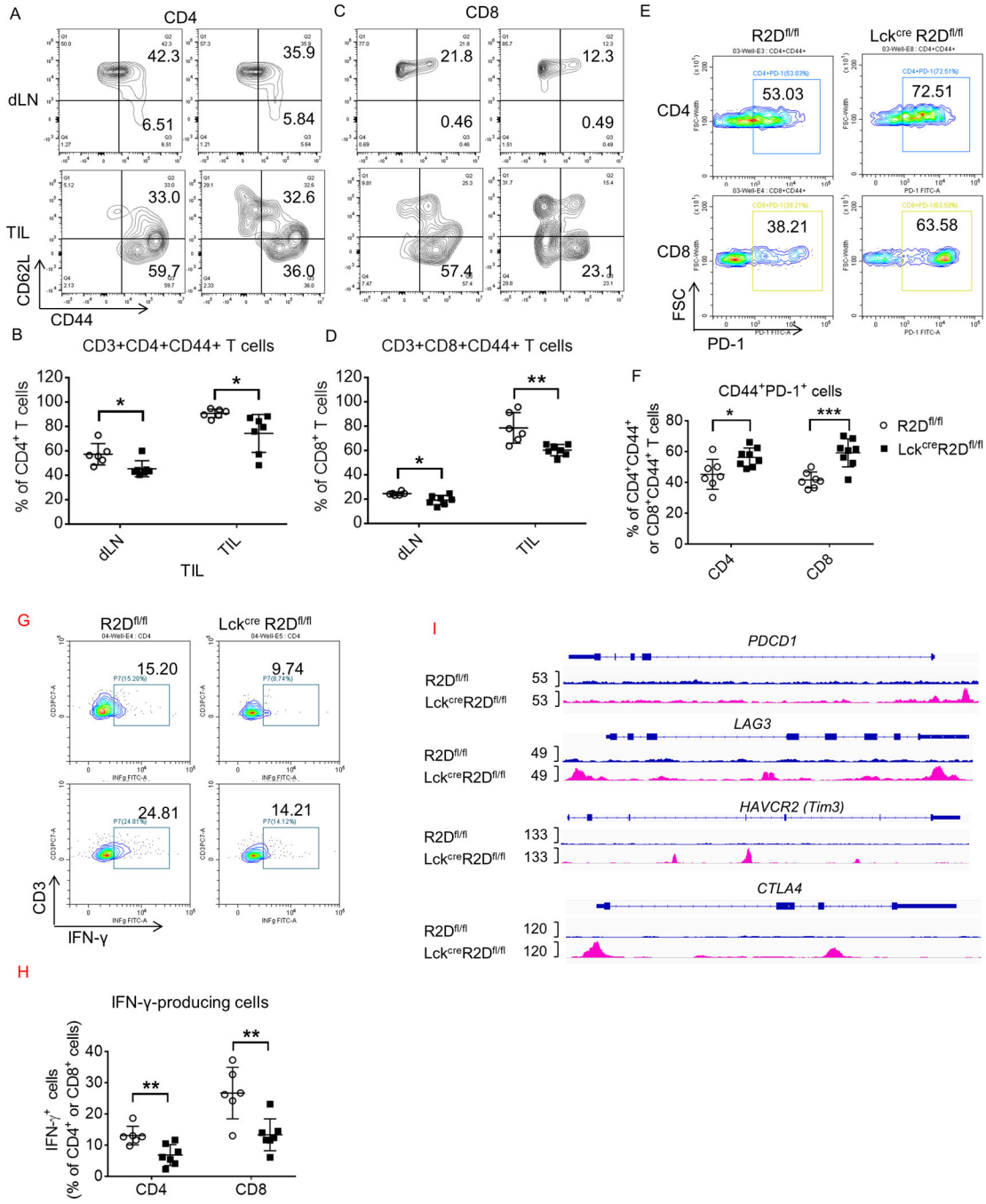

Figure 4. PPP2R2D deficiency in T cells increases the exhaustion of tumor-infiltrating T cells.

(**A-F**) B16-ova melanoma cells (2×10^5) were subcutaneously injected into $R2D^{fl/fl}$ (n = 6) or $Lck^{cre}R2D^{fl/fl}$ (n = 7) mice. On day 21 after injection of melanoma cells, mice were euthanized to collect tumors (**TIL**) and draining lymph nodes (**dLN**), and the lymphocytes were isolated, counted and analyzed by FACS staining. (**A-D**) Effector subsets ($CD3^+CD4^+CD44^+$ or $CD3^+CD8^+CD44^+$) as a percentage of $CD3^+CD4^+$ or $CD3^+CD8^+$ T cells in the dLN or TIL. The representative flow plots (**A** and **C**) and cumulative data (**B** and **D**) were shown. The representative plots (**E**) and cumulative

data (**F**) showing the percentages of $CD3^+CD4^+CD44^+PD1^+$ or $CD3^+CD8^+CD44^+PD1^+$ cells in $CD3^+CD4^+CD44^+$ or $CD3^+CD8^+CD44^+$ T cells from the TIL. (**G and H**) Representative flow plots (**G**) and cumulative data (**H**) showing the IFN-γ-producing cells ($CD3^+CD4^+$IFN-γ^+ or $CD3^+CD8^+$IFN-γ^+) as a percentage of $CD3^+CD4^+$ or $CD3^+CD8^+$ T cells in in the TIL. All the data were obtained from two independent experiments. **P<0.05, **P<0.01* and ****P<0.001* by multiple *T* test. (**I**) $CD4^+$ Tconv cells were sorted out from spleens of $R2D^{fl/fl}$ or $Lck^{Cre}R2D^{fl/fl}$ mice (n = 2 mice/group) and ex vivo stimulated by plate-bound CD3 and CD28 antibodies for 4 hours before being subjected to ATAC-seq. Accessibility tracks for selected gene loci *PDCD1*, *LAG3*, *HAVCR2* and *CTLA4*) in $R2D^{fl/fl}$ (up) and $Lck^{Cre}R2D^{fl/fl}$ (down) Tconv cells were plotted using the integrative genomics viewer (IGV).

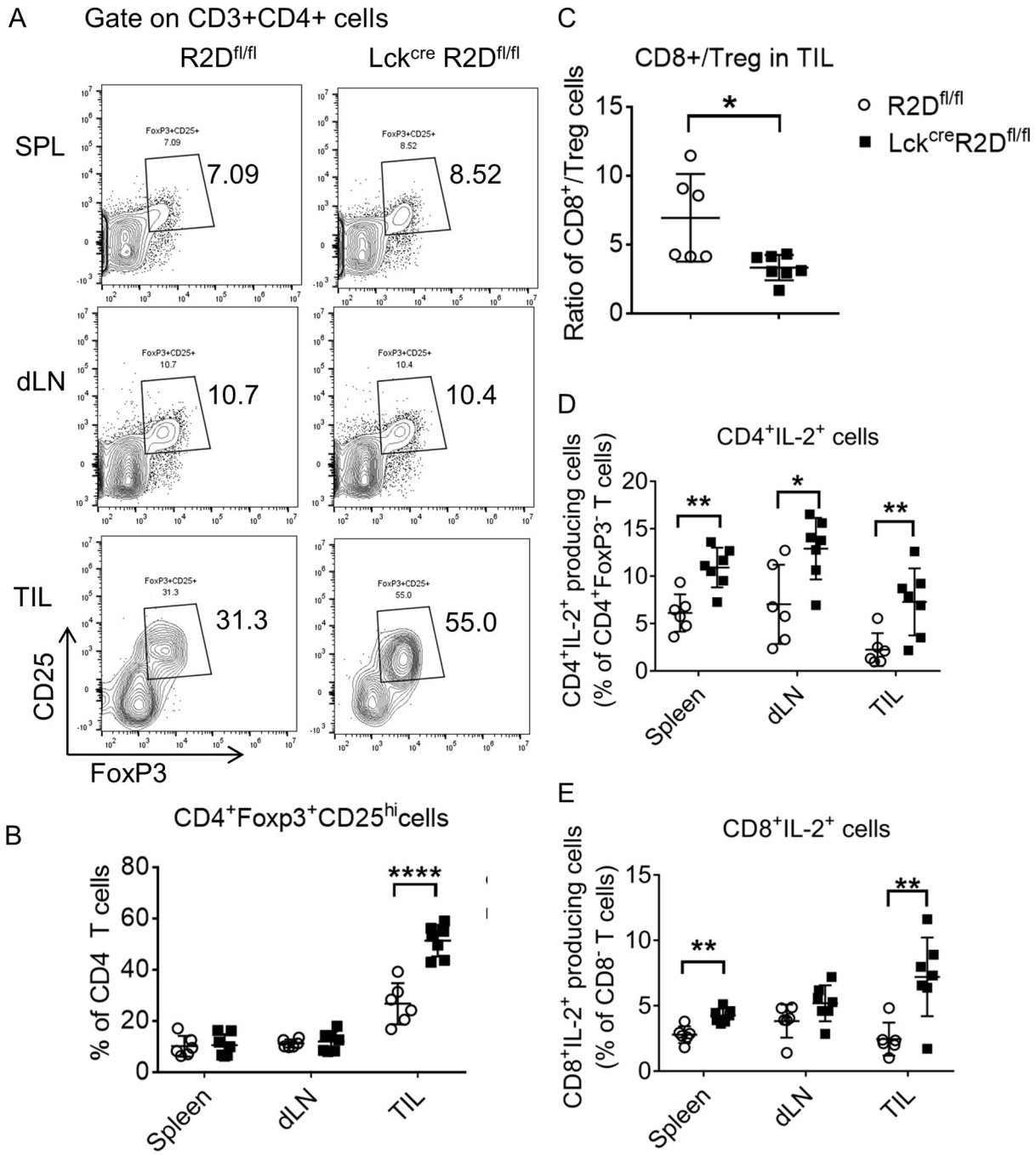

Figure 5. PPP2R2D deficiency in T cells increases Treg population in tumor-infiltrating T cells.

B16-ova melanoma cells (2×10^5) were subcutaneously injected into $R2D^{fl/fl}$ (n = 6) or $Lck^{cre}R2D^{fl/fl}$ (n = 7) mice. On day 21 after injection of melanoma cells, mice were euthanized to collect tumors (**TIL**), draining lymph nodes (**dLN**), and spleens (**SPL**), and the lymphocytes were isolated, counted and analyzed by FACS staining. (**A-B**) Treg cell subset ($CD3^+CD4^+Foxp3^+CD25^{hi}$) as a percentage of $CD3^+CD4^+$ T cells in the SPL, dLN or TIL. The representative flow plots (**A**) and cumulative data (**B**) were shown. (**C**) Ratio of CD8 ($CD3^+CD8^+$) and Treg cell subset ($CD3^+CD4^+Foxp3^+CD25^{hi}$) in the TIL. (**D-E**) IL-2-

producing cells (**D**: $CD3^+CD4^+IL\text{-}2^+$ or **E**: $CD3^+CD8^+IL\text{-}2^+$) as a percentage of $CD3^+CD4^+$ or $CD3^+CD8^+$ T cells in in the SPL, dLN or TIL. All the data were obtained from two independent experiments. **P<0.05, **P<0.01* and *****P<0.0001* by multiple *T* test.

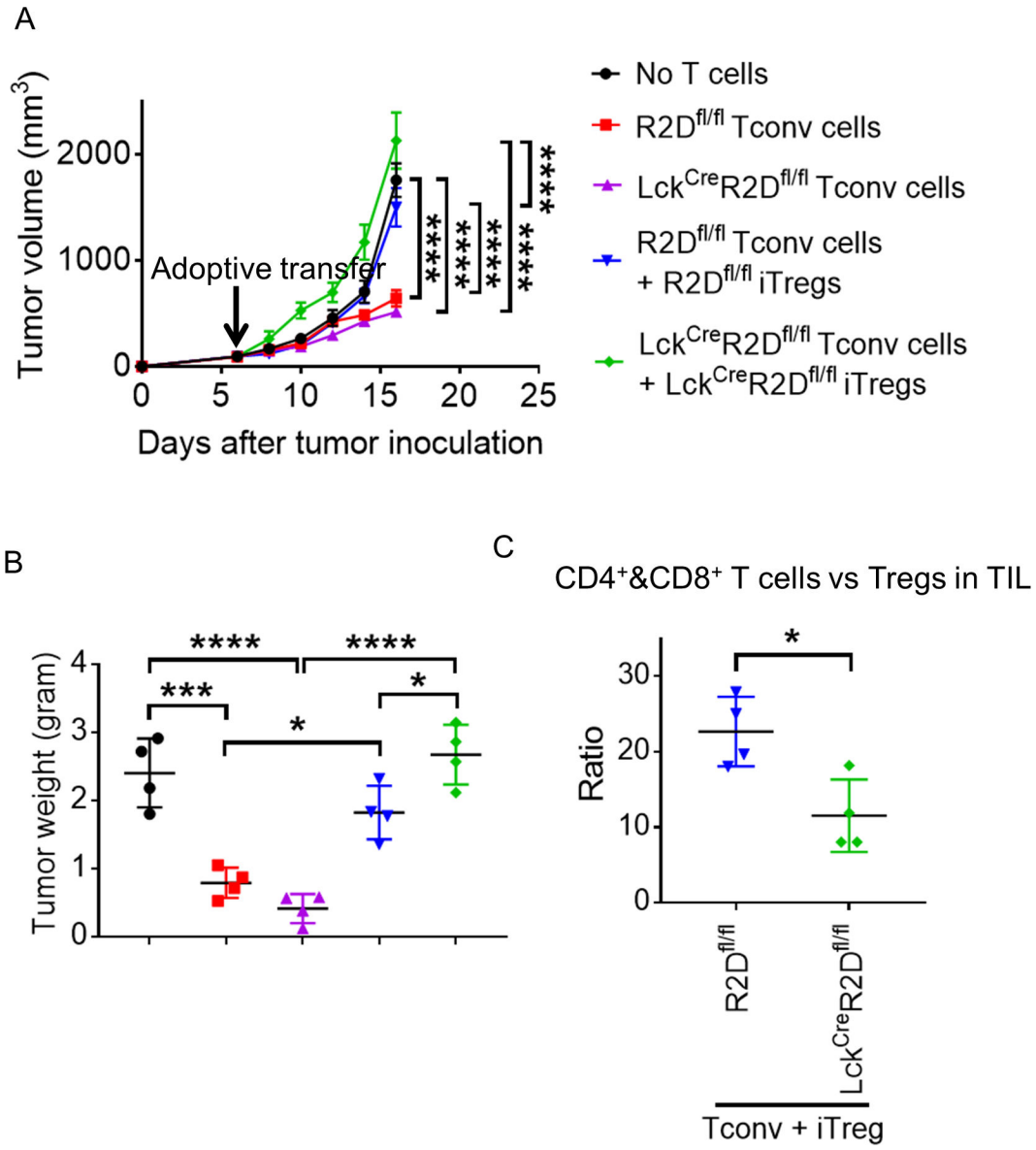

Figure 6. PPP2R2D deficiency in T cells enhanced the inhibitory effect of Treg cells on anti-tumor immunity.

B16-Ova tumor cells (2×10^5) were injected subcutaneously into Rag1 null ($Rag1^{-/-}$) mice (n= 4 mice per group). On day 6, mice bearing tumors of similar size were divided into 5 groups receiving: no T cells, $R2D^{fl/fl}$ CD4 and CD8 conventional T (Tconv) cells (2×10^6), $Lck^{cre}R2D^{fl/fl}$ CD4 and CD8 Tconv cells (2×10^6), $R2D^{fl/fl}$ CD4 and CD8 Tconv cells (2×10^6) plus $R2D^{fl/fl}$ inducible (i)Treg cells (0.25×10^6), or $Lck^{cre}R2D^{fl/fl}$ CD4 and CD8 Tconv cells (2×10^6) plus $Lck^{cre}R2D^{fl/fl}$ iTreg cells (0.25×10^6). (**A**) Tumor size was monitored every other day by measuring 3 diameters using digital caliper until day 18. (**B**) On day 18, mice were euthanized and tumors were collected and weighed. (**C**) Ratio of CD4 and CD8 ($CD3^+CD4^+$ and $CD3^+CD8^+$) and Treg cell subset ($CD3^+CD4^+Foxp3^+CD25^{hi}$) in the TIL. All the data were obtained from two independent experiments. **P<0.05 ***P<0.001*

*and ****P<0.0001* by two-way ANOVA with Holm-Šidákmultiple-comparisons test (**A**) or by unpaired *T* test (**B and C**).